

# A Light CNN for Deep Face Representation with Noisy Labels

Xiang Wu, Ran He, Zhenan Sun, Tieniu Tan

Center for Research on Intelligent Perception and Computing,

Institute of Automation, Chinese Academy of Sciences, Beijing, P. R. China, 100190

alfredxiangwu@gmail.com, {rhe, znsun, tnt}@nlpr.ia.ac.cn

## Abstract

Convolution neural network (CNN) has significantly pushed forward the development of face recognition and analysis techniques. Current CNN models tend to be deeper and larger to better fit large amounts of training data. When training data are from internet, their labels are often ambiguous and inaccurate. This paper presents a light CNN framework to learn a compact embedding on the large-scale face data with massive noisy labels. First, we introduce the concept of maxout activation into each convolutional layer of CNN, which results in a Max-Feature-Map (MFM). Different from Rectified Linear Unit that suppresses a neuron by a threshold (or bias), MFM suppresses a neuron by a competitive relationship. MFM can not only separate noisy signals and informative signals but also plays a role of feature selection. Second, a network of five convolution layers and four Network in Network (NIN) layers are implemented to reduce the number of parameters and improve performance. Lastly, a semantic bootstrapping method is accordingly designed to make the prediction of the models be better consistent with noisy labels. Experimental results show that the proposed framework can utilize large-scale noisy data to learn a light model in terms of both computational cost and storage space. The learnt single model with a 256-D representation achieves state-of-the-art results on five face benchmarks without fine-tuning. The light CNN model is released on [https://github.com/AlfredXiangWu/face\\_verification\\_experiment](https://github.com/AlfredXiangWu/face_verification_experiment).

## 1. Introduction

In the last decade, convolution neural network (CNN) has become one of the most popular techniques for computer vision. Numerous vision tasks, such as image classification [11], object detection [28], face recognition [33, 37, 43], have benefited from the robust and discriminative representation learnt via CNN models. Their performances have obtained great improvement, for example, the accu-

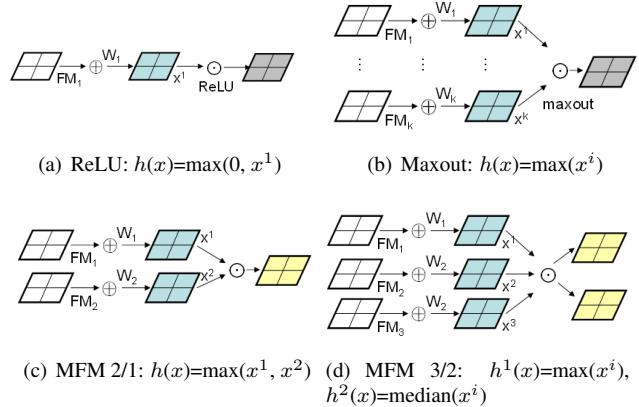


Figure 1. A comparison of different neural inhabitation. (a) ReLU suppresses a neuron by thresholding magnitude responses. (b) Maxout with enough hidden units makes a piecewise linear approximation to an arbitrary convex function. (c) MFM 2/1 suppresses a neuron by a competitive relationship. It is the simplest case of maxout activations. (d) MFM 3/2 activates two neurons and suppresses one neuron.

racy on the challenging LFW benchmark has been improved from 97% [37] to 99% [27, 30, 33]. This improvement is mainly due to the fact that CNN can learn a complex data distribution from the large-scale training datasets consisting of many identities. To achieve ultimate accuracy, the training dataset for CNN is becoming larger. Several face datasets have been published such as CASIA-WebFace [43], CelebFaces+ [33], VGG face dataset [27] and MS-Celeb-1M [10]. However, large-scale datasets often contain massive noisy labels especially when they are automatically collected from image search engines or movies.

This paper studies a light CNN framework to learn a deep face representation from the large-scale data with massive noisy labels. As shown in Fig. 1, we define a Max-Feature-Map (MFM) operation for a compact representation and feature filter selection. MFM is an alternative of ReLU to suppress low-activation neurons in each layer. It can be considered as a special implementation of max-

out activation [9] to separate noisy signals and informative signals. We implement the light CNN including MFM, small convolution filters and Network in Network, which is trained on the MS-Celeb-1M dataset. To handle noisy labeled images, we propose a semantic bootstrapping method to automatically re-label training data by the pre-trained deep networks. We assume that the consistency of the same predictions can be made by given similar percepts. Of course, too much skepticism of the original training label may lead to a wrong relabeling. Hence, it is important to balance the trade-off between the prediction and original label. Extensive experimental evaluations demonstrate that the proposed light CNN is effective and achieves state-of-the-art results on five face benchmarks without supervised fine-tuning. The contributions are summarized as follows:

- 1) This paper introduces MFM operation, a special case of maxout to learn a light CNN, which has a small number of parameters. Compared to ReLU whose threshold is learned from training data, MFM adopts a competitive relationship so that it has better generalization ability and is applicable for different data.
- 2) The light CNNs based on MFM are designed to learn a universal face representation. Convolution filters with small kernel size and Network in Network(NIN) are employed to reduce parameter space. These configurations lead to better performance in terms of speed and storage space.
- 3) A semantic bootstrapping method via a pretrained deep network is proposed to handle noisy labeled images in a large-scale dataset. Inconsistent labels can be effectively detected by the probabilities of predictions, and then are relabeled or removed for training.
- 4) The proposed single model with a 256-D representation obtains state-of-the-art results on five different face benchmarks, i.e., LFW [13], MegaFace [16], YTF [41], CACD-VS [3] and CASIA NIR-VIS 2.0 database [18]. The model contains about 5,556K parameters and extracts a face representation around 67ms (CPU time).

The paper is organized as follows. In Section 2, we briefly review some related work on face recognition and noisy label problems. Section 3 describes the proposed lighten CNN framework and the semantic bootstrapping method. Finally, we present experimental results in Section 4 and conclude this paper in Section 5.

## 2. Related Work

### 2.1. Face Recognition

Current face recognition methods are often based on CNN to obtain a robust feature extractor. Earlier DeepFace [37] trains CNN on 4.4M face images and uses CNN as a feature extractor for face verification. It achieves 97.35%

Table 1. The training datasets for face recognition.

Dataset	Available	subjects	images
CASIA-WebFace[43]	public	10K	500K
CelebFaces+[33]	public	10K	200K
VGG face dataset[27]	public	2.6K	2.6M
MS-Celeb-1M[10]	public	100K	8.4M
Facebook[37]	private	4K	4.4M
NTechLAB	private	200K	18M
Google[30]	private	10M	500M

accuracy on LFW with a 4096-D feature vector. As an extension of DeepFace, Web-Scale [38] applies a semantic bootstrapping method to select an efficient training set from a large dataset. It certifies that high dimensional feature vectors are not necessary for face recognition problems because the low dimensional features of Web-Scale can outperform DeepFace. And it also discusses more stable protocol [2] of LFW, which can indicate the robustness of face features more representatively. To further improve accuracy, Sun *et al.* [33] resorts to a multi-patch ensemble model. An ensemble of 25 CNN models is trained on different local patches and Joint Bayesian is applied to obtain a robust embedding space. In [35], verification loss and classification loss are further combined to increase inter-class distance and decrease intra-class distance. The ensemble model obtains 99.47% on LFW.

Recently, triplet loss is introduced into CNN, resulting in a new method named FaceNet [30]. FaceNet is trained on totally about 100-200M face images with 8M face identities. Since the selection of triplet pairs is important for accuracy, FaceNet presents an online triplet mining method for training triplet-based CNN and achieves good accuracy (99.63%). Then Parkhi *et al.* [27] combine the very deep convolution neural network [31] and the triplet embedding. They train the CNN model on 2622 identities of 2.6M images collected from Internet and then fine-tune the model via triplet-based metric learning method like FaceNet. The classification-based net obtains 97.27% and the deep embedding model achieves 98.95% on LFW.

The performance improvement of face recognition benefits from CNN and large-scale face datasets. As shown in Table 1, the published face databases are becoming larger. However, large-scale datasets often contain massive noisy labels especially when they are automatically collected from internet. Hence, how to learn a light CNN model from the large-scale face data with massive noisy labels becomes an important issue.

### 2.2. Noisy Label Problems

Noisy label is an important issue in machine learning when datasets tend to be large-scale. Many methods [7] are devoted to deal with noisy label problems. These meth-

ods can generally be classified into three categories. In the first category, robust loss [1, 23] is designed for classification tasks, so that the learnt classification models are robust to the presence of label noise. The second category [22, 40] aims to improve the quality of training data by identifying mislabeled instances. The third category [6, 17] directly models the distribution of noisy label during learning. The advantage of this approach allows using information about noisy labels during learning.

Recently, learning with noisy label data also draws much attention in deep learning, because deep learning is a data-driven approach and large-scale label annotation is quite expensive. Mnih and Hinton [24] introduce two robust loss functions for noisy label aerial images. However, their method is only applicable for binary classification. Sukhbaatar *et al.* [32] consider multi-class classification for modeling class dependent noise distribution. They propose a bottom-up noise model to change the label probabilities output for back-propagation and a top-down model to change given noisy labels before feeding data. Moreover, with the notion of perceptual consistency, the work of [29] extends the softmax loss function by weakly supervised training. The idea is to dynamically update the targets of the prediction objective function based on the current model. They use a simple convex combination of training labels and the predictions of a current model to generate training targets. Although some strategies have been studied for noisy label problem, massive noisy labels are still an ongoing issue for deep learning methods.

### 3. Architecture

In this section, we first propose Max-Feature-Map operation for CNN to simulate neural inhibition, resulting in a new light CNN framework for face analysis and recognition. Then, the semantic bootstrapping method for noisy labeled training dataset is addressed in detail.

#### 3.1. Max-Feature-Map Operation

Large-scale face training dataset often contains various types of noise and massive noisy labels. If the errors incurred by these noisy signals are not well treated, CNN will learn a bias result. Rectified Linear Unit (ReLU) [25] activation offers a way to separate noisy signals and informative signals. It makes use of a threshold (or bias) to determine the activation of one neuron. If the neuron is not active, its output value will be 0. However, this thresholding might lead to the loss of some information especially for the first several convolution layers because these layers are similar to Gabor filters (i.e., both positive and negative responses are respected). To alleviate this problem, the Leaky Rectified Linear Units (LReLU) [21], Parametric Rectified Linear Units (PReLU) [12] and Exponential Linear Units (ELU) [5] are proposed.

In neural science, lateral inhibition (LI) increases the contrast and sharpness in visual or audio response and aids the mammalian brain in perceiving contrast within an image. To take visual LI as an example, if an excitatory neural signal is released to horizontal cells, the horizontal cells will send an inhibitory signal to its neighboring or related cells. This inhibition produced by horizontal cells creates a more concentrated and balanced signal to cerebral cortex. To take auditory LI as an example, if certain sound frequencies create a greater contribute to inhibition than excitation, tinnitus can be suppressed. Considering LI and noisy signals, we expect the activation function in one convolution layer to have the following characters:

- 1) Since large-scale dataset often contains various types of noise, we expect that noisy signals and informative signals can be separated.
- 2) When there is a horizontal edge or line in an image, the neuron corresponding to horizontal information is excited whereas the neuron corresponding to vertical information is inhibited.
- 3) The inhabitation of one neuron is parameter free so that it does not depend on training data very much.

To achieve the above characters, we propose the Max-Feature-Map (MFM) operation, which is an extension of Maxout activation [9]. Different from Maxout activation that uses enough hidden neurons to approximate an arbitrary convex function, MFM suppresses only a small number of neurons to make CNN models light and robust. We define two MFM operations to obtain competitive feature maps.

Given an input convolution layer  $x^n \in \mathbb{R}^{H \times W}$ , where  $n = \{1, \dots, 2N\}$ ,  $W$  and  $H$  denote the spatial width and height of the feature map. The MFM 2/1 operation which combines two feature maps and outputs element-wise maximum one as shown in Fig. 1(c) can be written as

$$\hat{x}_{ij}^k = \max(x_{ij}^k, x_{ij}^{k+N}) \quad (1)$$

where the channel of the input convolution layer is  $2N$ ,  $1 \leq k \leq N$ ,  $1 \leq i \leq H$ ,  $1 \leq j \leq W$ . As is shown in Eq. (1), the output  $\hat{x}$  via MFM operation belongs to  $\mathbb{R}^{H \times W \times N}$ .

The gradient of Eq.(1) takes the following form,

$$\frac{\partial \hat{x}_{ij}^k}{\partial x^{k'}} = \begin{cases} 1, & \text{if } x_{ij}^k \geq x_{ij}^{k+N} \\ 0, & \text{otherwise} \end{cases} \quad (2)$$

where  $1 \leq k' \leq 2N$  and

$$k = \begin{cases} k' & 1 \leq k' \leq N \\ k' - N & N + 1 \leq k' \leq 2N \end{cases} \quad (3)$$

Considering MFM 2/1, we mainly obtain 50% informative neurons from input feature maps via the element-wise maximum operation across feature channels.

Furthermore, as shown in Fig. 1(d), to obtain more comparable feature maps, the MFM 3/2 operation, which inputs three feature maps and removes element-wise minimum one, can be defined:

$$\begin{cases} \hat{x}_{ij}^{k_1} = \max(x_{ij}^k, x_{ij}^{k+N}, x_{ij}^{k+2N}) \\ \hat{x}_{ij}^{k_2} = \text{median}(x_{ij}^k, x_{ij}^{k+N}, x_{ij}^{k+2N}) \end{cases} \quad (4)$$

where  $x^n \in \mathbb{R}^{H \times W}$ ,  $1 \leq n \leq 3N$ ,  $1 \leq k \leq N$  and median() is the middle value of input feature maps. The gradient of MFM 3/2 is similar to Eq. (3), in which the value of gradient is 1 when the feature map  $x_{ij}^k$  is activated, and it tends to be 0 otherwise. In this way, we select and reserve 2/3 information from input feature maps.

### 3.2. The Light CNN Framework

When MFM operation is introduced to CNN, it performs a similar role of the feature selection of local features in biometrics. It selects the best feature at the same location learnt by different filters. It results in binary gradient (0 and 1) to excite or suppress one neuron during back propagation. The binary gradient plays a similar role of ordinal measure [36] that is famous local feature and widely used in biometrics.

The CNN with MFM can obtain a compact representation while the gradient of MFM layer is sparse. Due to the sparse gradient, on the one hand, when doing back propagation for training CNN, the processing of stochastic gradient descent (SGD) can only make effects on the neuron of response variables. On the other hand, when extracting features for testing, MFM can obtain more competitive nodes from previous convolution layers by activating the maximum of two feature maps. These appearances result in the properties that MFM can perform feature selection and sparse connection in our light CNN models.

In addition, since Network in Network (NIN) can potentially do feature selection between convolution layers and small convolution kernel can reduce the number of parameters for a model [31], we integrate NIN and small convolution kernel size into the network with MFM. Finally, the proposed light CNN contains 5 convolution layers, 4 Network in Network (NIN) layers [19], Max-Feature-Map layers, 4 max-pooling layers and 2 fully connected layers. Its detail is presented in Table 2.

An input image is  $144 \times 144$  gray-scale face image from the training dataset. We crop each input image randomly into  $128 \times 128$  patch as the input of the first convolution layer for training. Each convolution layer is combined with two independent convolution parts calculated from its input. Max-Feature-Map layer and max pooling layer are used later. The fc1 layer is a 256-dimensional face representation. The fc2 layer is used as the input of the softmax cost function and is simply set to the number of training set identities.

Table 2. The architectures of the light CNN model.

Type	Filter Size /Stride	Output Size	#Params
Conv1	$5 \times 5/1, 2$	$128 \times 128 \times 96$	2.4K
MFM1	-	$128 \times 128 \times 48$	-
Pool1	$2 \times 2/2$	$64 \times 64 \times 48$	-
Conv2a	$1 \times 1/1$	$64 \times 64 \times 96$	4.6K
MFM2a	-	$64 \times 64 \times 48$	-
Conv2	$3 \times 3/1, 1$	$64 \times 64 \times 192$	165K
MFM2	-	$64 \times 64 \times 96$	-
Pool2	$2 \times 2/2$	$32 \times 32 \times 96$	-
Conv3a	$1 \times 1/1$	$32 \times 32 \times 192$	18K
MFM3a	-	$32 \times 32 \times 96$	-
Conv3	$3 \times 3/1, 1$	$32 \times 32 \times 384$	331K
MFM3	-	$32 \times 32 \times 192$	-
Pool3	$2 \times 2/2$	$16 \times 16 \times 192$	-
Conv4a	$1 \times 1/1$	$16 \times 16 \times 384$	73K
MFM4a	-	$16 \times 16 \times 192$	-
Conv4	$3 \times 3/1, 1$	$16 \times 16 \times 256$	442K
MFM4	-	$16 \times 16 \times 128$	-
Conv5a	$1 \times 1/1$	$16 \times 16 \times 256$	32K
MFM5a	-	$16 \times 16 \times 128$	-
Conv5	$3 \times 3/1, 1$	$16 \times 16 \times 256$	294K
MFM5	-	$16 \times 16 \times 128$	-
Pool4	$2 \times 2/2$	$8 \times 8 \times 128$	-
fc1	-	512	4,194K
MFM_fc1	-	256	-
Total	-	-	5,556K

### 3.3. Semantic Bootstrapping for Noisy Label

Bootstrapping, also called "self-training", provides a simple means for sample estimation. It is widely used to estimate a sampling distribution due to its simplicity and effectiveness. Its basic idea is that the inference about a training sample can be modeled by re-sampling and performing inference from original labeled samples to re-labeled them. It can estimate standard errors and confidence intervals for a complex data distribution and it is also appropriate to control the stability of the estimation.

Let  $x \in X$  and  $t$  be the data and their labels, respectively. The CNN based on softmax loss function regresses  $x$  onto  $t$ , which its prediction can be represented as a conditional probability  $p(t|f(x))$ ,  $\sum_i p(t_i|f(x)) = 1$ . Obviously, the maximum probability  $p(t_i|f(x))$  determines the prediction label and is more confident, especially for a large number of subjects.

Due to the observations, we propose a semantic bootstrapping method to sample the training data from the large dataset with massive noisy label. Firstly, we train a light CNN model on the original noisy labeled dataset. The MFM operation potentially leads to robustness for the property of perceptual consistency for training because the gra-

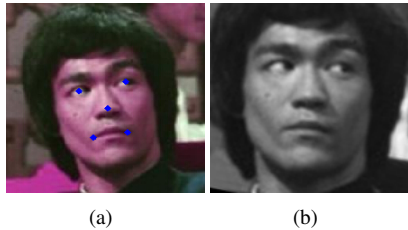


Figure 2. Face image alignment for WebFace dataset. (a) is the facial points detection results and (b) is the normalized face image.

dient of MFM is sparse. Therefore the light CNN model can converge stably even if there are lots of the noisy labeled data in the training dataset. Secondly, we employ the trained model to predict the labels of noisy labeled training dataset. And then we set a threshold to decide whether accept or reject the prediction according to the conditional probabilities  $p(t_i|f(x))$ . Finally, we retrain the light CNN model on the re-labeled training dataset. The details for bootstrapping the MS-Celeb-1M dataset are shown in Section 4.5.

## 4. Experiments

In this section, we evaluate our light CNN models on various face recognition tasks. We first introduce the training methodology and databases, and then present the comparison with state-of-the-art face recognition methods, as well as algorithmic analysis and detailed evaluation. Finally, we discuss the effectiveness of the semantic bootstrapping method for selecting training dataset.

### 4.1. Training Methodology and Preprocessing

To train the light CNN, we randomly select one face image from each identity as the validation set and the remaining images as the training set. The open source deep learning framework *Caffe* [14] is employed to train the CNN model. Dropout is used for fully connected layers and the ratio is set to 0.7. The momentum is set to 0.9, and the weight decay is set to 5e-4 for convolution layers and a fully-connected layer except the fc2 layer. Obviously, the fc1 fully-connected layer contains the face representation that can be used for face verification. Note that, the number of the parameters from fc1 layer to fc2 layer is very large. But these parameters are not used for feature extractor. Therefore, they may lead to over-fit if the large fully-connected layer parameters are learnt. To overcome this over-fitting, we set the weight decay of fc2 layer to 5e-3. The learning rate is set to 1e-3 initially and reduced to 5e-5 gradually. The parameter initialization for convolution is Xavier and Gaussian is used for fully-connected layers.

The CASIA-WebFace and MS-Celeb-1M datasets (see Table 1) are used to train our light convolution neural net-

works. All face images are converted to gray-scale and normalized to  $144 \times 144$  via landmarks as shown in Fig. 2(a). The normalized face image is shown in Fig. 2(b). According to the 5 facial points extracted by [34] and manual adjustment, we rotate two eye points to be horizontal, which can overcome the pose variations in roll angle. The distance between the midpoint of eyes and the midpoint of mouth, as well as the y axis of midpoint of eyes, are set to 48 pixels for training set, for the distance between the midpoint of eyes and the midpoint of mouth is relatively invariant to pose variations in yaw angle. Since the input  $144 \times 144$  image is randomly cropped into  $128 \times 128$  for the first convolution input, the y axis of midpoint of eyes is set to 48 for training and 40 for testing, respectively.

### 4.2. The Testing Protocols

Five face databases are used to systematically evaluate the performance of the proposed light CNN. These databases corresponds to large-scale, low-resolution, cross-age and heterogeneous face recognition (or verification) tasks respectively. **Note that we do not re-train or fine-tune the light CNN model on any testing database.** That is all the training sets in the five databases are not used for training or fine-tuning. We directly extract the features of the light CNN learnt on the MS-Celeb-1M dataset and compute the similarity of these features in cosine similarity.

The first testing database is the commonly used LFW dataset [13] that contains 13,233 images of 5,749 people. For the verification protocol [13], face images are divided in 10 folds which contain different identities and 600 face pairs. In unrestricted setting, the identities within each fold for training are allowed to be much larger. For the probe-gallery identification testing [2], there are two new protocols called the close set and open set identification tasks. 1) For the close set task, the gallery contains 4,249 identities, each with only a single face image, and the probe set contains 3,143 face images belonging to the same set of identities. The performance is measured by Rank-1 identification accuracy. 2) For the open set task, the gallery set includes 3,143 images of 596 identities. The probe set includes 10,090 images which are constructed by 596 genuine probes and 9,494 impostor ones. The accuracy is evaluated by the Rank-1 Detection and Identification Rate (DIR), which is genuine probes matched in Rank-1 at a 1% False Alarm Rate (FAR) of impostor ones that are not rejected.

The second testing database is the very challenging MegaFace database [16] that aims at the evaluation of face recognition algorithms at million-scale. It includes probe and gallery set. The probe set is FaceScrub [26], which contains 100K images of 530 identities, and the gallery set consists of about 1 million images from 690K different subjects. As in [39], we evaluate the proposed light CNN by the

Table 3. Comparison with other state-of-the-art methods on the LFW verification and identification protocol. The unrestricted protocol follows the LFW unrestricted setting and the unsupervised protocol means the model is not trained on LFW in supervised way.

Method	#Net	Accuracy	VR@FAR=0	Protocol	Rank-1	DIR@FAR=1%
DeepFace [37]	7	97.35%	46.33%	unrestricted	64.90%	44.50%
Web-Scale [38]	1	98.00%	-	unrestricted	82.10%	59.20%
Web-Scale [38]	4	98.37%	-	unrestricted	82.50%	61.90%
DeepID2+ [35]	1	98.70%	-	unrestricted	-	-
DeepID2+ [35]	25	99.47%	<b>69.36%</b>	unrestricted	<b>95.0%</b>	<b>80.7%</b>
WebFace+Joint Bayes [43]	1	97.73%	-	unrestricted	-	-
FaceNet [30]	1	<b>99.63%</b>	-	unrestricted	-	-
SeetaFace [20]	1	98.60%	59.00%	unrestricted	91.95%	63.26%
SeetaFace(Full) [20]	1	98.62%	-	unrestricted	92.79%	68.13%
DeepFace [37]	1	95.92%	-	unsupervised	-	-
VGG [27]	1	97.27%	52.40%	unsupervised	74.10%	52.01%
CenterLoss [39]	1	98.70%	61.40%	unsupervised	<b>94.05%</b>	69.97%
MFM 2/1	1	<b>98.80%</b>	<b>94.97%</b>	unsupervised	93.80%	<b>84.40%</b>

provided code<sup>1</sup>, which only tests on one of the three gallery set (set 1) for both face identification and face verification protocols.

The third testing database is the YouTube Face (YTF) database [41] that is widely used to evaluate the performance of video-based face recognition methods. It contains 3,425 videos of 1,595 different people. Due to low resolution and motion blur, the quality of images in the YTF dataset is worse than LFW. For the evaluation protocol, the YTF dataset is divided into 10 splits. Each split includes 250 positive pairs and 250 negative ones. As in [27, 30], we randomly select 100 samples from each video and compute the average similarities.

The fourth testing database is the CACD-VS dataset [3] that contains large variations in aging. It includes 4,000 image pairs (2000 positive pairs and 2000 negative pairs) by collecting celebrity images on Internet.

The final testing database is the largest public and challenging CASIA NIR-VIS 2.0 database [18] for heterogeneous face recognition. It consists of different modality face images. We follow the standard protocol in View 2. There are 10 fold experiments and each fold contains 358 subjects in the testing set. For testing, the gallery set contains only 358 VIS images for each subjects and the probe set consist of 6,000 NIR images from the same 358 subjects.

### 4.3. Method Comparison

In this subsection, we compare the proposed light CNN with state-of-the-art methods according to the testing protocols in Section 4.2. For one private business method, we directly report its results from its published paper. For the published method whose source code of feature extraction is available, we extract its deep features and then report its results based on these features. Since the computational

cost of the feature extraction of SeetaFace [20] is high, we do not report its results on some databases. Tables 3-7 show the results of different methods on the five face databases. We have the following observations.

The proposed light CNN method achieves better and comparable results than its competitors. Although it performs lower than several private business methods on the LFW and MegaFace, it outperforms the published methods, including VGG [27], CenterLoss [39] and SeetaFace [20]. It is one of the best published CNN methods for face recognition. Note that when MFM 3/2 is used for our light CNN method, the performance on the LFW database can be further improved (Table 8). As shown in the following Section 4.3, our light CNN has a small model size and only use a 256-D feature representation to achieve the best results.

On the LFW database (as shown in Table 3), our model trained on MS-1M-2R obtains 98.80% with unsupervised setting, which means our model is not trained or fine-tuned on the LFW training dataset in a supervised way. The results of our model on the LFW verification protocol are better than those of DeepFace [37], DeepID2+ [35], WebFace [43], VGG [27], CenterLoss [39] and SeetaFace [20] for a single net. Although several business methods have achieved ultimate accuracy on 6000-pairs face verification task, the more practical criterion may be the verification rate at the extremely low false acceptance rate (eg., VR@FAR=0). We achieve 94.97% at VR@FAR=0, while other methods' results are lower than 70%. Moreover, open-set identification rate at low false acceptance rate is even more challenging but applicable. As shown in Table 3, we obtain 84.40% which outperforms DeepFace, DeepID2+, VIPLFaceNet, CenterLoss and VGG. These results suggest that our light CNN learns more discriminative embedding than other CNN methods.

<sup>1</sup><http://megaface.cs.washington.edu/participate/challenge.html>

Table 4. MegaFace performance comparison with other methods on rank-1 identification accuracy with 1 million distractors and verification TAR for  $10^{-6}$  FAR.

Method	Rank-1	VR@FAR= $10^{-6}$
NTechLAB	73.300%	85.081%
FaceNet v8 [30]	70.496%	86.473%
Beijing Faceall Co. 3DiVi Company	64.803% 33.705%	67.118% 36.927%
Barebones.FR	59.363%	59.036%
CenterLoss [39]	65.234%	76.510%
MFM 2/1	65.532%	75.854%
MFM 2/1 mirror	<b>67.109%</b>	<b>77.456%</b>

Table 5. Comparison with other state-of-the-art methods on Youtube Face dataset.

Method	#Net	Accuracy
DeepFace [37]	1	91.40%
WebFace+PCA [43]	1	90.60%
VGG [27]	1	92.80%
DeepID2+ [35]	25	93.20%
FaceNet [30]	1	<b>95.10%</b>
CenterLoss [39]	1	94.90%
MFM 2/1	1	93.40%

On the MegaFace database (as shown in Table 4), we compare the light CNN against FaceNet [30], NTechLAB, CenterLoss [39], Beijing Faceall Co., Barebones.FR and 3DiVi Company. To improve the robustness of our algorithm, we extract the features for each image and its horizontal mirror one, and then concatenate them as the representation followed by [39]. The light CNN achieves **67.109%** on rank-1 accuracy and **77.456%** on VR@FAR= $10^{-6}$  which outperforms Barebones FR, CenterLoss, and even commercial face recognition methods (Beijing Faceall Co. and 3DiVi Company). Besides, note that the Google FaceNet and NTechLAB achieve better performance than our model due to the large-scale private training dataset (500M for Google and 18M for NTechLAB) and unknown preprocessing techniques.

Table 5 and Table 6 show the results on the YouTube Face (YTF) dataset and the CACD-VS dataset respectively. Due to low resolution and motion blur, the quality of images in YTF is worse than LFW. Our light CNN obtains 93.40% by using a single model, which outperforms the results of DeepFace, VGG and WebFace without fine-tuning on YTF. The usage of low-resolution face images in the training set may further improve the robustness of our lightened model. The result of our model on CACD-VS is 97.95% and outperforms other age-invariant face recognition algorithms [3, 4, 8] and two open source models [27, 20]. This indicates that our light CNN is potentially robust for age-variant problems.

It is interesting to observe that our light CNN also per-

Table 6. Accuracy of different methods on CACD-VS.

Method	Accuracy
HD-LBP [4]	81.60%
HFA [8]	84.40%
CARC [3]	87.60%
VGG [27]	96.00%
SeetaFace [20]	95.50%
MFM 2/1	<b>97.95%</b>
Human, Average	85.70%
Human, Voting	94.20%

Table 7. Rank-1 accuracy and VR@FAR=0.1% of different methods on CASIA 2.0 NIR-VIS Face Database.

Method	Rank-1	VR@FAR=0.1%
Gabor+RBM [42]	$86.16 \pm 0.98\%$	$81.29 \pm 1.82\%$
DLBP [15]	$78.46 \pm 1.67\%$	$85.80\%$
VGG [27]	$62.09 \pm 1.88\%$	$39.72 \pm 2.85\%$
SeetaFace [20]	$68.03 \pm 1.66\%$	$58.75 \pm 2.26\%$
CenterLoss [39]	$87.69 \pm 1.45\%$	$69.72 \pm 2.07\%$
MFM 2/1	<b><math>91.88 \pm 0.58\%</math></b>	<b><math>85.31 \pm 0.95\%</math></b>

forms very well on the NIR-VIS dataset. It not only outperforms the three CNN methods but also significantly improves state-of-the-art results. We improve the best rank-1 accuracy from  $86.16\% \pm 0.98\%$  to  **$91.88\% \pm 0.58\%$**  and the VR@FAR=0.1% is further improved from  $81.29\% \pm 1.82\%$  to  **$85.31\% \pm 0.95\%$** . Note that all CNN methods are not fine-tuned on the NIR-VIS dataset. The improvement of our light CNN may benefit from its character of parameter free in an activation function. Our MFM 2/1 depends on a competitive relationship rather than a threshold of ReLU so that it is naturally adaptive to different appearances from different modalities.

All of the experiments suggest that the proposed light CNN obtains discriminative face representations and has good generalization for various face recognition tasks.

#### 4.4. Network Analysis

MFM plays an important role in our lightened CNN. Hence we give a detailed analysis of MFM in this subsection. We compare the performance of MFM 2/1 and MFM 3/2 with ReLU, PReLU and ELU on the LFW database. To simplify the computation of MFM 3/2, we employ  $h^1(c) = \max(c^1, c^2)$ ,  $h^2(c) = \max(c^2, c^3)$  to approximate Eq. (4). Although this approximation will induce some redundancy, experimental results show that this approximation can further improve verification rates. The experimental results of different activation functions are shown in Table 8.

We observe that the CNN with MFM 3/2 achieves the highest performance in terms of accuracy, rank-1 and DIR-FAR=1%. For our lightened CNN, MFM 3/2 and MFM 2/1 are superior to the three other activation functions. This may be due to the fact that our MFM uses a competitive relation-

Table 8. Comparison with different activation functions on LFW verification and identification protocol.

Method	Accuracy	Rank-1	DIR@FAR=1%
ReLU [25]	98.30%	88.58%	67.56%
PReLU [12]	98.17%	88.30%	66.30%
ELU [5]	97.70%	84.70%	62.09%
MFM 2/1	98.80%	93.80%	84.40%
MFM 3/2	<b>98.83%</b>	<b>94.97%</b>	<b>88.59%</b>

Table 9. The time cost and the number of parameters of our model compared with VGG release model and SeetaFace. The speed is tested on a single core i-7 4970.

Model	#Param	#Dim	Times
VGG [27]	134,251K	4096	581ms
VIPLFaceNetFull [20]	50,021K	2048	245ms
VIPLFaceNet [20]	35,582K	2048	150ms
CenterLoss [39]	19,596K	1024	160ms
Our model	5,556K	256	67ms

ship rather than a threshold (or bias) to active a neuron. Since the training and testing sets are from different data sources, MFM has better generalization ability to different sources. Compared with MFM 2/1, MFM 3/2 can further improve performance. This indicates that when using MFM, it would be better to keep only a small number of neurons to be inhibited so that more information can be preserved to the next convolution layer. That is, the ratio between input neurons and output neurons is set to between 1 and 2.

Very deep convolution neural networks or multi-patch ensemble are common ways to improve recognition accuracy. But they are often time consuming for practical systems. Computational efficiency is also an important issue for CNN models. To verify the computational efficiency of our light CNN, we compare our CNN with three public CNNs, i.e., the VGG released model [27], open source SDK SeetaFace [20] and CenterLoss [39].

As shown in Table 9, the size of our light CNN model is 20 times smaller than that of the well-known VGG model, while the CPU time is about 9 times faster. Compared with the open source face SDK SeetaFace and CenterLoss, our light CNN also performs well in terms of time cost, the number of parameters and feature dimension. The results indicate that our light CNN is potentially suitable and practical on embedding devices and smart phones for real-time applications than its competitors. Particularly, these results also suggest that MFM (as a special case and extension of Maxout activation) can result in a convolution neural network with a small parameter space and a small feature dimension. If MFM is well treated and carefully designed, the learnt CNN can use smaller parameter space to achieve better recognition accuracy.

Table 10. The performance on **VAL1** and **VAL2** for different database trained model. It compares the performance of light CNN model trained on CASIA-WebFace, MS-Celeb-1M, MS-Celeb-1M after 1 times bootstrapping(MS-1M-1R) and MS-Celeb-1M after 2 times bootstrapping(MS-1M-2R). The area under Precision-Recall curve(AUC) and verification rate(VR)@fasle acceptance rate(FAR) for different models are shown.

VAL1	AUC	FAR=0.1%	FAR=0.01%
CASIA	89.72%	92.50%	84.82%
MS-Celeb-1M	92.03%	94.42%	88.48%
MS-1M-1R	94.82%	96.86%	92.15%
MS-1M-2R	95.34%	97.03%	93.54%
VAL2	AUC	FAR=0.1%	FAR=0.01%
CASIA	62.82%	62.84%	44.46%
MS-Celeb-1M	75.79%	77.93%	61.38%
MS-1M-1R	81.04%	82.66%	68.91%
MS-1M-2R	82.94%	84.55%	71.39%

#### 4.5. Noisy Label Data Bootstrapping

In this subsection, we verify the efficiency of the proposed semantic bootstrapping method on the MS-Celeb-1M database. The tests are performed on two datasets in which face images are subject variations in viewpoint, resolution and illumination. The first dataset, denoted as VAL1, contains 1,424 face images of 866 identities. The second dataset contains 675 identities and totally 3,277 images, which is denoted as VAL2. There are 573 positive pairs and 1,012,603 negative pairs (i.e., totally 1,013,176 pairs) in VAL1. VAL2 contains 2,632,926 pairs that are composed of 4,015 positive and 2,628,911 negative pairs. All the face images in VAL1 and VAL2 are independent from the CASIA-WebFace and MS-Celeb-1M database. Considering highly imbalance dataset evaluations, we employ Receiver Operator Characteristic (ROC) curves and Precision-Recall (PR) curves to evaluate the performance of the retrain models via bootstrapping. Both on VR@FAR for ROC curves and AUC for PR curves are reported.

First, we train a light CNN model on the CASIA-WebFace database that contains 10,575 identities totally about 50K images. Then, we fine-tune our light CNN on MS-Celeb-1M, initialized by the pre-trained model on CASIA-WebFace. Since MS-Celeb-1M contains 99,891 identities, the fully-connected layer from feature representation (256-d) to identity label, which is treated as the classifier, has a large number of parameters ( $256 \times 99,891 = 25,572,096$ ). To alleviate the difficulty of CNN convergence, we firstly set the learning rate of all the convolution layers to 0. The softmax loss only contributes to the last fully-connected layer to train the classifier. When it converges coarsely, the learning rate of all the convolution layers is set to the same. And then the learning rate is gradually decreased from 1e-3 to 1e-5.

Second, we employ the trained model in the first step to predict the MS-Celeb-1M dataset and obtain the probability  $\hat{p}_i$  and  $\hat{t}_i$  for each sample  $x_i \in X$ . Since the abilities of perceptual consistency can be influenced by the noisy labeled data in the training set, the strict bootstrapping rules are employed to select samples. We accept the re-labeling sample whose prediction label  $\hat{t}$  is the same as the ground truth label  $t$  and whose probability  $\hat{p}_i$  is upper than the threshold  $p_0$  which is set to 0.7. In this way, the MS-Celeb-1M re-labeling dataset, defined as MS-1M-1R, contains 79,077 identities totally 4,086,798 images.

Third, MS-1M-1R is used to retrain the light CNN model following the training methodology in Section 4.1. Furthermore, the original noisy labeled MS-Celeb-1M database is re-sampled by the model trained on MS-1M-1R. Assuming that there are few noisy labeled data in MS-1M-1R, we accept the following samples: 1) The prediction  $\hat{t}$  is the same as ground truth label  $t$ ; 2) The prediction  $\hat{t}$  is different from the ground truth label  $t$ , but the probability  $p_i$  is upper than the threshold  $p_1$  which is set to 0.7. The dataset after bootstrapping, which contains 5,049,824 images for 79,077 identities, denoted as MS-1M-2R.

Finally, we retrain the light CNN on MS-1M-2R. Table 10 shows experimental results of the CNN models learnt on different subsets. We have the following observations: 1) The MS-Celeb-1M database contains massive noisy labels. If the noisy labels are well treated, the performances on the two testing datasets can be improved. Our proposed semantic bootstrapping method provides a practical way to deal with the noisy labels on the MS-Celeb-1M database. 2) Verification performance benefits from the larger dataset. The model trained on the original MS-Celeb-1M database with noisy labels outperforms the model trained on the CASIA-WebFace database in terms of both ROC and AUC. 3) After two bootstrapping steps, the number of identities is from 99,891 to 79,077 and performance improvement tends to be small. These indicate that our semantic bootstrapping method can obtain a better dataset to train our CNN.

## 5. Conclusions

In this paper, we have developed a light convolution neural network framework to learn a robust face representation on noisy labeled dataset. Inspired by neural inhabitation and maxout activation, we proposed a Max-Feature-Map operation to obtain a compact and low dimensional face representation. Small kernel sizes of convolution layers and Network in Network layers have been implemented to reduce parameter space and improve performance. One advantage of our framework is that it is faster and smaller than other published CNN methods. It extracts one face representation by using about 67ms on a single core i7-4790, and it only occupies 5,556K parameters. Besides, an effective semantic bootstrapping has been proposed to handle the noisy label

problem. Experimental results on various face recognition datasets show that the proposed light CNN framework has potential value for some real-time face recognition systems.

## References

- [1] E. Beigman and B. B. Klebanov. Learning with annotation noise. In *Proceedings of Annual Meeting of the Association for Computational Linguistics*, pages 280–287, 2009.
- [2] L. Best-Rowden, H. Han, C. Otto, B. Klare, and A. K. Jain. Unconstrained face recognition: Identifying a person of interest from a media collection. *IEEE Transactions on Information Forensics and Security*, 9(12):2144–2157, 2014.
- [3] B. Chen, C. Chen, and W. H. Hsu. Face recognition and retrieval using cross-age reference coding with cross-age celebrity dataset. *IEEE Transactions on Multimedia*, 17(6):804–815, 2015.
- [4] D. Chen, X. Cao, F. Wen, and J. Sun. Blessing of dimensionality: High-dimensional feature and its efficient compression for face verification. In *Proceedings of the IEEE Conference on Computer Vision and Pattern Recognition*, pages 3025–3032, 2013.
- [5] D. Clevert, T. Unterthiner, and S. Hochreiter. Fast and accurate deep network learning by exponential linear units (elus). *CoRR*, abs/1511.07289, 2015.
- [6] T. Denoeux. A neural network classifier based on dempster-shafer theory. *IEEE Transactions on Systems, Man, and Cybernetics, Part A*, 30(2):131–150, 2000.
- [7] B. Frénay and M. Verleysen. Classification in the presence of label noise: A survey. *IEEE Transactions on Neural Networks and Learning Systems*, 25(5):845–869, 2014.
- [8] D. Gong, Z. Li, D. Lin, J. Liu, and X. Tang. Hidden factor analysis for age invariant face recognition. In *Proceedings of the IEEE International Conference on Computer Vision*, pages 2872–2879, 2013.
- [9] I. J. Goodfellow, D. Warde-Farley, M. Mirza, A. C. Courville, and Y. Bengio. Maxout networks. In *Proceedings of International Conference on Machine Learning*, pages 1319–1327, 2013.
- [10] Y. Guo, L. Zhang, Y. Hu, X. He, and J. Gao. Ms-celeb-1m: A dataset and benchmark for large-scale face recognition. *CoRR*, abs/1607.08221, 2016.
- [11] K. He, X. Zhang, S. Ren, and J. Sun. Deep residual learning for image recognition. *CoRR*, abs/1512.03385, 2015.
- [12] K. He, X. Zhang, S. Ren, and J. Sun. Delving deep into rectifiers: Surpassing human-level performance on imagenet classification. *CoRR*, abs/1502.01852, 2015.
- [13] G. B. Huang, M. Ramesh, T. Berg, and E. Learned-Miller. Labeled faces in the wild: A database for studying face recognition in unconstrained environments. Technical report, Technical Report 07-49, University of Massachusetts, Amherst, 2007.
- [14] Y. Jia, E. Shelhamer, J. Donahue, S. Karayev, J. Long, R. B. Girshick, S. Guadarrama, and T. Darrell. Caffe: Convolutional architecture for fast feature embedding. In *Proceedings of the ACM International Conference on Multimedia*, pages 675–678, 2014.

[15] F. Juefei-Xu, D. K. Pal, and M. Savvides. NIR-VIS heterogeneous face recognition via cross-spectral joint dictionary learning and reconstruction. In *Proceedings of the IEEE Conference on Computer Vision and Pattern Recognition Workshops*, pages 141–150, 2015.

[16] I. Kemelmacher-Shlizerman, S. M. Seitz, D. Miller, and E. Brossard. The megaface benchmark: 1 million faces for recognition at scale. In *Proceedings of the IEEE Conference on Computer Vision and Pattern Recognition*, 2016.

[17] N. D. Lawrence and B. Schölkopf. Estimating a kernel fisher discriminant in the presence of label noise. In *Proceedings of International Conference on Machine Learning*, pages 306–313, 2001.

[18] S. Z. Li, D. Yi, Z. Lei, and S. Liao. The CASIA NIR-VIS 2.0 face database. In *Proceedings of the IEEE Conference on Computer Vision and Pattern Recognition Workshops*, pages 348–353, 2013.

[19] M. Lin, Q. Chen, and S. Yan. Network in network. *CoRR*, abs/1312.4400, 2013.

[20] X. Liu, M. Kan, W. Wu, S. Shan, and X. Chen. ViPLFaceNet: An open source deep face recognition sdk. *Frontiers of Computer Science*, 2016.

[21] A. L. Maas, A. Y. Hannun, and A. Y. Ng. Rectifier nonlinearities improve neural network acoustic models. In *Proceedings of International Conference on Machine Learning*, volume 30, 2013.

[22] A. Malossini, E. Blanzieri, and R. T. Ng. Detecting potential labeling errors in microarrays by data perturbation. *Bioinformatics*, 22(17):2114–2121, 2006.

[23] N. Manwani and P. S. Sastry. Noise tolerance under risk minimization. *IEEE Transactions on Cybernetics*, 43(3):1146–1151, 2013.

[24] V. Mnih and G. E. Hinton. Learning to label aerial images from noisy data. In *Proceedings of the 29th International Conference on Machine Learning*, 2012.

[25] V. Nair and G. E. Hinton. Rectified linear units improve restricted boltzmann machines. In *Proceedings of International Conference on Machine Learning*, pages 807–814, 2010.

[26] H. Ng and S. Winkler. A data-driven approach to cleaning large face datasets. In *Proceedings of the IEEE International Conference on Image Processing*, pages 343–347, 2014.

[27] O. M. Parkhi, A. Vedaldi, and A. Zisserman. Deep face recognition. *Proceedings of the British Machine Vision Conference*, 2015.

[28] J. Redmon, S. K. Divvala, R. B. Girshick, and A. Farhadi. You only look once: Unified, real-time object detection. *CoRR*, abs/1506.02640, 2015.

[29] S. E. Reed, H. Lee, D. Anguelov, C. Szegedy, D. Erhan, and A. Rabinovich. Training deep neural networks on noisy labels with bootstrapping. *CoRR*, abs/1412.6596, 2014.

[30] F. Schroff, D. Kalenichenko, and J. Philbin. Facenet: A unified embedding for face recognition and clustering. In *Proceedings of the IEEE Conference on Computer Vision and Pattern Recognition*, pages 815–823, 2015.

[31] K. Simonyan and A. Zisserman. Very deep convolutional networks for large-scale image recognition. *CoRR*, abs/1409.1556, 2014.

[32] S. Sukhbaatar and R. Fergus. Learning from noisy labels with deep neural networks. *CoRR*, abs/1406.2080, 2014.

[33] Y. Sun, Y. Chen, X. Wang, and X. Tang. Deep learning face representation by joint identification-verification. In *Proceedings of Advances in Neural Information Processing Systems 27*, pages 1988–1996, 2014.

[34] Y. Sun, X. Wang, and X. Tang. Deep convolutional network cascade for facial point detection. In *Proceedings of the IEEE Conference on Computer Vision and Pattern Recognition*, pages 3476–3483, 2013.

[35] Y. Sun, X. Wang, and X. Tang. Deeply learned face representations are sparse, selective, and robust. In *Proceedings of the IEEE Conference on Computer Vision and Pattern Recognition*, pages 2892–2900, 2015.

[36] Z. Sun and T. Tan. Ordinal measures for iris recognition. *IEEE Transactions on Pattern Analysis and Machine Intelligence*, 31(12):2211–2226, 2009.

[37] Y. Taigman, M. Yang, M. Ranzato, and L. Wolf. Deepface: Closing the gap to human-level performance in face verification. In *Proceedings of the IEEE Conference on Computer Vision and Pattern Recognition*, pages 1701–1708, 2014.

[38] Y. Taigman, M. Yang, M. Ranzato, and L. Wolf. Web-scale training for face identification. In *Proceedings of the IEEE Conference on Computer Vision and Pattern Recognition*, pages 2746–2754, 2015.

[39] Y. Wen, K. Zhang, Z. Li, and Y. Qiao. A discriminative feature learning approach for deep face recognition. In *Proceedings of the European Conference on Computer Vision*, pages 499–515. Springer, 2016.

[40] D. R. Wilson and T. R. Martinez. Instance pruning techniques. In *Proceedings of International Conference on Machine Learning*, pages 403–411, 1997.

[41] L. Wolf, T. Hassner, and I. Maoz. Face recognition in unconstrained videos with matched background similarity. In *Proceedings of the IEEE Conference on Computer Vision and Pattern Recognition*, pages 529–534, 2011.

[42] D. Yi, Z. Lei, and S. Z. Li. Shared representation learning for heterogenous face recognition. In *Proceedings of IEEE International Conference and Workshops on Automatic Face and Gesture Recognition*, pages 1–7, 2015.

[43] D. Yi, Z. Lei, S. Liao, and S. Z. Li. Learning face representation from scratch. *CoRR*, abs/1411.7923, 2014.